THE ALGEBRAIC RECONSTRUCTION TECHNIQUE (ART)*

D.Raparia, J.Alessi, and A.Kponou
AGS Department, Brookhaven National Lab, Upton, NY 11973, USA

Abstract

Projections of charged particle beam current density (profiles) are frequently used as a measure of beam position and size. In conventional practice only two projections, usually horizontal and vertical, are measured. This puts a severe limit on the detail of information that can be achieved. A third projection provides a significant improvement. The Algebraic Reconstruction Technique (ART) uses three or more projections to reconstruct 3-dimensional density profiles. At the 200 MeV H- linac, we have used this technique to measure beam density, and it has proved very helpful, especially in helping determine if there is any coupling present in x-y phase space. We will present examples of measurements of current densities using this technique.

1 INTRODUCTION

In Computed Tomography (CT), three dimensional reconstruction techniques from projection have been used for many years in radiology. The two dimensional Fourier transform is the most commonly used algorithm in radiology. In this technique a large number of projections at uniformly distributed angles around the subject are required for reconstruction of the image. In the field of accelerator physics, one expects that the relatively simple charged particle beam distributions can be reconstructed from a small number of projections. In conventional practice only two projections, usually horizontal and vertical, are measured. This puts a severe limit on the level of detail that can be achieved. The Algebraic Reconstruction Technique (ART) introduced by Gordan, Bender and Herman [1] uses three or more projections to reconstruct the 2-dimensional beam density distribution. They have shown that the improvement in the quality of the reconstruction is pronounced when a third projection is added, but additional projections add much less to the reconstruction quality.

2 ALGEBRAIC RECONSTRUCTION TECHNIQUE (ART)

The ART algorithms have a simple intuitive basis. Each projected density is thrown back across the reconstruction space in which the densities are iteratively modified to bring each reconstructed projection into agreement with the measured projection. Assuming that the pattern being reconstructed is enclosed in a square space of n x n array of small pixels, $\rho_j \left(j = 1, \ldots, n^2\right)$ is grayness or density number, which is uniform within the pixel but different from other pixels. A "ray" is a region of the square space which lies between two parallel lines. The weighted ray sum is the total grayness of the reconstruction figure within the ray. The projection at a given angle is then the sum of non-overlapping, equally wide rays covering the figure. The ART algorithm consists of altering the grayness of each pixel intersected by the ray in such a way as to make the ray sum agree with the corresponding element of the measured projection. Assume **P** is a matrix of m x n^2 and the m component column vector **R.** Let $p_{i,j}$ denote the (i,j)th element of **P** , and R_i denote the ith ray of the reconstructed projection vector **R**. For $1 \leq i \leq m$, N_i is number of pixels under projection ray R_i, defined as $N_i = \sum_{j=1}^{n^2} p_{i,j}^2$. ART is an iterative method. The density number ρ_j^q denotes the value of ρ_j after q iterations. After q iterations the intensity of the ith reconstructed projection ray is

$$R_i^q = \sum_{j=1}^{n^2} p_{i,j} \rho_j^q,$$

and the density in each pixel is

$$\rho_j^{\sim q+1} = \rho_j^q + p_{i,j} \frac{R_i - R_i^q}{N_i} \quad \text{with starting value } \rho_j^{\sim 0} = 0$$

where R_i is the measured projection ray and,

$$i = \begin{cases} \text{m, if (q+1) is divisible m} \\ \text{the remainder of dividing (q+1)by m, otherwise} \end{cases}$$

and,

$$\rho_j^q = \begin{cases} 0, & \text{if } \rho^{\sim q} \leq 0 \\ \rho_j^{\sim q}, & \text{if } 0 \leq \rho_j^{\sim q} \leq 1 \\ 1, & \text{if } \rho_j^{\sim q} \geq 1 \end{cases}$$

This algorithm is known as fully constrained ART.

It is necessary to determine when an iterative algorithm has converged to a solution which is optimal according to some criterion. Various criteria for convergence have been devised. The discrepancy between the measured and calculated projection elements is

$$D^q \equiv \left\{ \frac{1}{m} \sum_{i=1}^{m} \frac{(R_i - R_i^q)^2}{N_i} \right\}^{\frac{1}{2}},$$

and the nonuniformity or variance of constructed figure is

$$V^q \equiv \sum_j \left(\rho_j^q - \overline{\rho}\right)^2,$$

and the entropy constructed figure is

$$E^q \equiv \frac{-1}{2 \log n} \sum_j \left(\frac{\rho_j^q}{\overline{\rho}}\right) \log \left(\frac{\rho_j^q}{\overline{\rho}}\right).$$

* Work performed under the auspices of the U. S. Department of Energy.

D^q tends to zero, V^q to a minimum and S^q to a maximum with increasing q. For a known test pattern ($\rho^t_{i,j}$), the Euclidean Distance is define as

$$s^q \equiv \sqrt{\frac{1}{n^2}\sum_j \left(\rho^q_j - \rho^t_j\right)^2}.$$

3 TEST FIGURE

It is instructive to test the reconstruction capabilities of ART with two to four views by using projections from a known test figure. In the following example, we have used an x-y coupled (about 18°)two-dimensional gaussian enclosed in a square space of 100 x 100 array with $\sigma_x = 5$ and $\sigma_y = 20$. We have used a ray width in the 45° and 135° projection as $\sqrt{2}$ times of ray width in x or y projection, making number of ray in each projection same namely 100. Fig. 1 shows the test figure and reconstructed test figure from two projections. Fig. 2 shows reconstructed test figure from three and four projections.

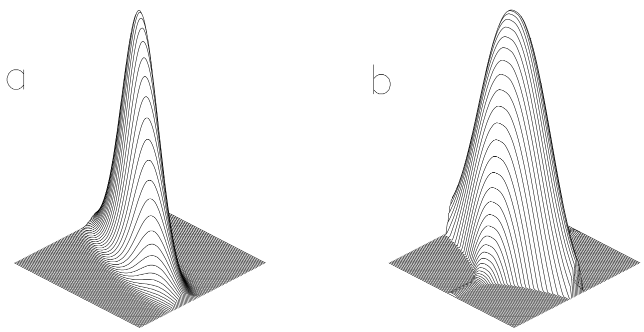

Figure 1: (a) Original test figure and (b) reconstructed test figure from two projections.

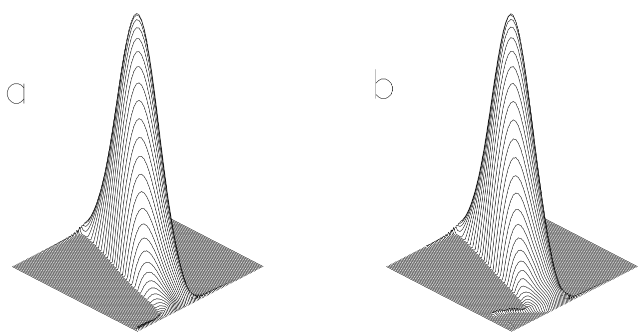

Figure 2: Reconstructed test figures from (a) three and (b) four projections.

Fig. 3 shows the contours of Figures 1 and 2. It is clear from Fig. 3 that two projections are not enough for catching the coupling. The accuracy of the reconstructed figure from four projection is slightly better than three projections. Fig. 4 shows the discrepancy (D), variance (V), the entropy (E) and the Euclidean Distance (s) as a function of iteration number for case of three projections. The

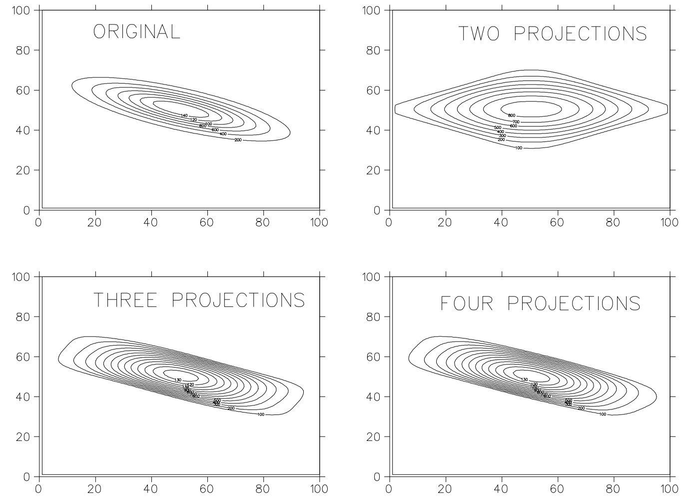

Figure 3: Contour plots of test figure and reconstructed figures with two, three and four projections.

Table 1: The convergence criteria discrepancy (D), variance (V), the entropy (E) and the Euclidean Distance (s) for two, three and four projections.

	2 Proj.	3 Proj.	4 Proj.
Iteration No	67	1426	1083
Time (sec)	201	6393	6534
Discrepancy	$1.0\ 10^{-6}$	$1.0\ 10^{-6}$	$1.0\ 10^{-6}$
Variance	$4.8\ 10^{-8}$	$1.3\ 10^{-8}$	$1.3\ 10^{-8}$
Entropy	$1.9\ 10^{+3}$	$2.3\ 10^{+3}$	$2.4\ 10^{+3}$
E. Distance	$1.5\ 10^{-4}$	$4.6\ 10^{-5}$	$4.6\ 10^{-5}$

convergence criteria was if discrepancy is less than 10^{-6}. Table 1 show the numerical values of discrepancy (D), variance (V), the entropy (E) and the Euclidean Distance (s) for two, three and four projections.

4 BEAM DENSITY MEASUREMENT

There are stepping wire profile scanners at 13 locations throughout the 200 MeV linac and transport lines. These scanners are mounted at a 45° angle with respect to horizontal, and single horizontal and vertical wires are stepped through the bea We have added a third wire at 45° to horizontal in two of the scanners, one in the 750 keV line [2] and one in the 200 MeV BLIP [3] transport line. Fig. 5 shows a schematic of the scanner with three wires. Fig. 6 shows the reconstructed density distributions at 750 keV line. There is no x-y coupling in the 750 keV line. Fig. 7 shows beam density contour plots in the BLIP line. The x-y coupling is clearly seen. This coupling could come from one or more rotated quadrupoles or vertical beam offset in a dipole. In the presence of x-y coupling, the usual tech-

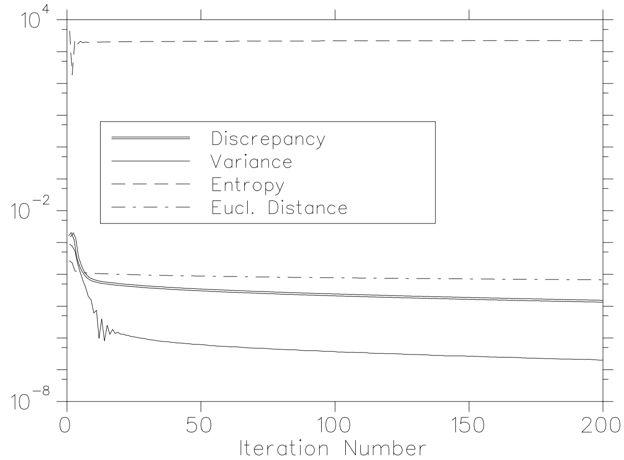

Figure 4: The discrepancy (D), variance (V), entropy (E) and the Euclidean Distance (s) as a function of iteration number for case of three projections. The convergence criteria was if discrepancy is less the 10^{-6}.

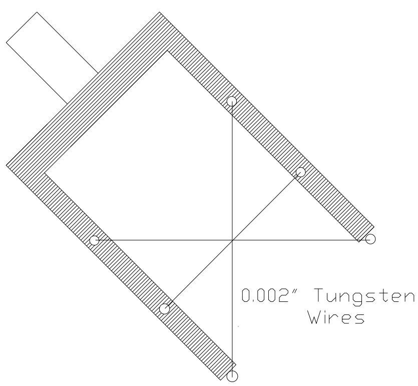

Figure 5: Schematic of the scanner with three wires.

nique of emittance measurement from profiles at three or more locations will not work. Figure 8 compares the measured and reconstructed projections in the BLIP line.

5 REFERENCES

[1] R. Gordon, *et at* "Three-Dimensional Reconstruction from Projections: A Review of Algorithms", International Review of Cytology, Vol. 38, pp 111 (1974)

[2] J. G. Alessi, *et al*, " Upgrade of the Brookhaven 200 MeV Linac", Proceedings of the XVII International Linear Accelerator Conference, Geneva, Switzerland ,26-30 August 1996, pp 773.

[3] A. Kponou, *et al*, " A New Optical Design for the BNL Isotope Production Transport Line", Proceedings of the XVII International Linear Accelerator Conference, Geneva, Switzerland ,26-30 August 1996, pp 770.

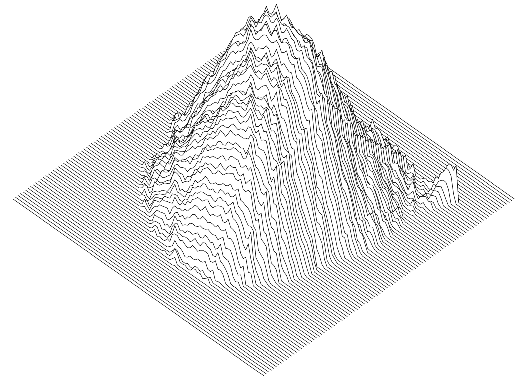

Figure 6: Reconstructed 3D density distribution in the 750 keV line using ART.

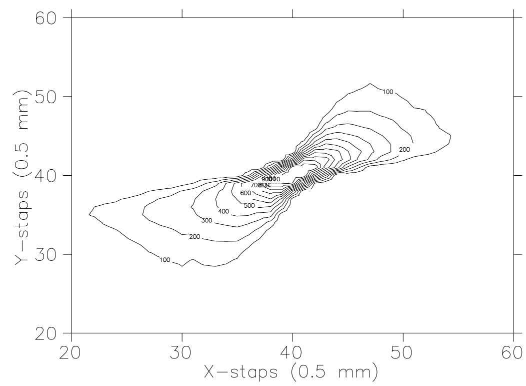

Figure 7: Reconstructed contour plot using ART in the BLIP line, showing x-y coupling.

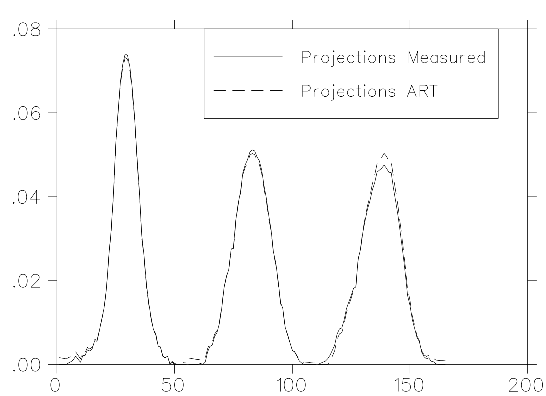

Figure 8: Beam projection measured and reconstructed on X, Y, and 45° planes at BLIP line.